Climate Dynamics (2022) 58:2767–2780
https://doi.org/10.1007/s00382-021-06032-z

Improvement of summer precipitation simulation by correcting biases of spring soil moisture in the seasonal frozen-thawing zone over the Northern Hemisphere

Kechen Li[1] · Feimin Zhang[1] · Kai Yang[1] · Jiali Shen[1] · Chenghai Wang[1]

Received: 28 April 2021 / Accepted: 25 October 2021 / Published online: 1 November 2021

Abstract
Soil moisture (SM) plays an important role in the climate system, and the effects of SM anomalies on climate can persist from month to season. The seasonal frozen-thawing zone (SFTZ) in the northern hemisphere (NH), which is associated with large inter-annual variability in spring SM, is important from land–atmosphere interaction perspective. In this study, by assimilating spring SM in the SFTZ through indirect soil nudging (ISN) in the Weather Research and Forecasting (WRF) model, the effects of correcting spring SM biases in the SFTZ on subsequent summer precipitation simulations in the NH are investigated. The results indicated that correcting spring SM biases in the SFTZ improves the subsequent summer precipitation simulations in the NH. Correcting spring SM biases in the SFTZ significantly adjusts energy and moisture evolution on the land surface from spring to summer. Specifically, the correction of SM biases by assimilating SM in SFTZ in the spring can clearly reduce the biases of sensible heat flux (SH) and latent heat flux (LH) in the summer. This affects land–atmosphere interactions over NH, leading to correcting the negative biases of the geopotential height in the middle troposphere in June and July, as well as larger biases of water vapor transport and its divergence during the summer. The results imply that spring SM in the SFTZ is a potential signal for predicting summer precipitation in the NH.

Keywords Soil moisture · Seasonal freeze–thaw region · Indirect soil nudging · Precipitation simulation

1 Introduction

Land–atmosphere interactions play a critical role in climate variation. Soil moisture (SM) variability changes surface albedo and soil heat capacity, which affect the surface sensible heat flux (SH), latent heat flux (LH), and radiation budget (e.g., Amenu et al. 2005; Song et al. 2009). Additionally, SM variability regulates precipitation and evapotranspiration by altering the surface water balance (e.g., Bounoua and Krishnamurti 1993; Wu et al. 2002). SM anomalies contribute to climate variations on the sub-seasonal to seasonal scale owing to its long-lasting effects (e.g., Koster et al. 2004; Li et al. 2016; Seneviratne et al. 2006a, b, 2013; Wang et al. 2003, 2020; Yang et al. 2019a, b). In the mid-latitudes of the Northern Hemisphere (NH), effect of SM on climate is more distinct than it is in the low or high latitudes, in terms of increased distance from the ocean (Yeh et al. 1984; Seneviratne et al. 2006a, b, 2010). This means that the variability of atmospheric circulation in the mid-latitudes of the NH is mainly affected by land–atmosphere interactions besides thermodynamic force from the low and high latitudes. The statistical analysis suggests that the seasonal frozen-thawing zone (SFTZ) in the NH shows the largest inter-annual variability in spring SM (Yang et al. 2016). This suggests that the characteristics and patterns of atmospheric circulation will be changed by the significant SM anomalies induced by freeze–thaw processes in soil when air passes through the mid-latitude SFTZ during the spring (Yang et al. 2016; Yang and Wang 2019a; Jiang and Wang 2020). Therefore, the spring SM variation that primarily induced by frozen-thawing processes in the SFTZ over NH has special significance. However, there is large uncertainty in SM simulation and reanalysis data, due to deficiency of parameterization scheme in land surface model.

✉ Chenghai Wang
wch@lzu.edu.cn

[1] Key Laboratory of Climate Resource Development and Disaster Prevention of Gansu Province, Research and Development Centre of Earth System Model, College of Atmospheric Sciences, Lanzhou University, Lanzhou 730000, Gansu Province, China

Observation and simulation suggested that SM has biases over SFTZ in NH (e.g., Koster et al. 2010; Ferguson et al. 2012b; Nicolai-Shaw et al. 2015; Prodhomme et al. 2016). Realistic description of spring SM in the SFTZ is crucial for the climate prediction. SM sensitive experiments have suggested that SM anomalies affect precipitation on daily to monthly time scales, regionally and globally (e.g., Walker and Rowntre 1977; Shukla and Mintz 1982; Douville et al. 2001; Douville 2002). Studies have further suggested that more realistic SM initialization and evolution in the models can improve the prediction of precipitation on sub-seasonal and seasonal time scales (e.g., Koster et al. 2004, 2010; Vitart et al. 2008; Douville 2009; Prodhomme et al. 2016; Wang and Cui 2018). Meanwhile, Yang et al. (2016) perturbed the initial SM in a series of sensitivity experiments and provides evidence that the spring SM anomaly in the SFTZ could lead to subsequent summer precipitation anomalies in the NH. However, there are some issues remain to address. How to ensure the reasonable initial condition by decreasing SM biases in the SFTZ? How to correct spring SM biases in the SFTZ, and what impacts would be on the subsequent climate simulation? Understanding these issues can benefit to improving climate model performance.

The pervasive SM biases exist in current databases such as reanalysis databases (Ni-Meister et al. 2005; Yang et al. 2016). SM biases in initial conditions and boundary conditions (ICBCs) would further induce unrealistic long-term evolution of SM, which would lead to inaccurate climate simulation. An effective approach to improve accuracy of SM in land surface models is assimilating observed SM data. The problem with assimilating SM data in the root zone arises from the lack of in situ SM observations globally, especially in the SFTZ. Although satellite-based SM observations have become increasingly available in recent years, the observed depth of most of them is under 10 cm, and the data quality is significantly affected by differences in soil texture, landscape, vegetation coverage, and precipitation (Gao et al. 2006; Kerr et al. 2012). Furthermore, numerical models have been used to improve the spatiotemporal resolution of SM data, but the SM simulation performance was not consistent between different models owing to flawed model parameters (Guo and Dimeyer 2006; Dirmeyer 2011). In the Pleim–Xiu land surface model (PXLSM), Pleim and Xiu (2003) proposed the indirect soil nudging (ISN) assimilation scheme, which used differences in 2 m air temperature (T_{2m}) and 2 m relative humidity (RH_{2m}) between models and observations to continuously correct SM tendencies in model. Meanwhile, nudging coefficients are computed according to model parameters rather than from statistical analysis, which reflect potential for the surface and root-zone SM to affect near-surface air temperature and humidity. ISN dynamically adjusts the SM by continuous nudging according to the realistic model biases and nudging strengths. Wang and Cui (2018) provided evidence that SM assimilation using ISN improved short-term climate predictions in China. Thus, ISN is a reliable method for SM assimilation in the SFTZ. Considering the evident SM biases in SFTZ (Yang et al. 2016), the contribution of correcting spring SM in the SFTZ to summer precipitation predictions remains unclear. On this basis, this study aims to evaluate the summer precipitation simulation through correcting spring SM in the SFTZ and to explain the possible mechanisms.

Three main issues will be addressed: (1) Can spring SM biases in the SFTZ be corrected by nudging scheme? (2) Can summer precipitation simulations in the NH be improved by correcting spring SM biases over the SFTZ? (3) What are the possible mechanisms linked to the improvement in summer precipitation simulations by correcting spring SM biases over the SFTZ? Answering these issues will improve our knowledge on the large-scale and non-local effects of SM in the SFTZ and SM initialization in regions without in situ SM observations on precipitation in the NH.

The remainder of this study is organized as follows: Sect. 2 provides a brief description of the model, data, and experiment design. Section 3 shows the corrected spring SM simulation biases after assimilating spring SM in the SFTZ. Section 4 shows the validation of summer precipitation simulation performance after correcting spring SM biases. Section 5 shows the changes in land surface elements by correcting spring SM biases in the SFTZ. Section 6 discusses the possible mechanisms behind the improvement of precipitation simulation in the NH. Section 7 provides conclusions and overall findings of the study.

2 Data and methods

2.1 Model and data

The Advanced Research version of the Weather Research and Forecasting Model (WRF-ARW, version 3.9.1) was used in this study. The ICBCs were provided by National Centers for Environmental Prediction (NCEP) final (FNL) analysis data with spatial and temporal resolutions of $1^\circ \times 1^\circ$ and 6 h, respectively. FNL data continuously collects observational data from various sources including the Global Telecommunications System (GTS) which is the product of Global Forecast System (GFS). Observed T_{2m} and RH_{2m} interpolated from objective analysis were originated from global surface observational weather data (spatial resolution: $0.5^\circ \times 0.5^\circ$; temporal resolution: 6 h) with automatic data processing (ADP) provided by the NCEP. This ADP dataset includes wind reports from the GTS, profiler and U.S. radar-derived winds, and SSM/I oceanic winds and satellite wind data from the National Environmental Satellite, Data, and Information Service (NESDIS). Due to the absence of observations in the

whole NH, SM SH, and LH data obtained from ERA-Interim (spatial resolution: 0.5° × 0.5°; temporal resolution: 6 h), ERA5 (spatial resolution: 0.5° × 0.5°; temporal resolution: 1 h), and the Noah land surface model from the Global Land Data Assimilation System (GLDAS) version 2.1 (spatial resolution: 0.25° × 0.25°; temporal resolution: 3 h) was used for simulation verification (Dee et al. 2011; Hersbach et al 2020; Chen et al. 1996; Koren et al. 1999). ERA-Interim, ERA5 and GLDAS2.1 Noah datasets are based on observations from many source and advanced assimilation system. SM, SH, and LH data from these datasets can well represent temporal and spatial characteristics of SM, SH, and LH, while the comparisons against observations in some regions also demonstrate the reasonability of these datasets (e.g., Zhang et al. 2008; Ferguson et al. 2012a; Decker, et al. 2012; Liu et al. 2014; Wang et al. 2016; Liu et al. 2021). Additionally, the ERA5 dataset was also used to compare the simulation results of geopotential height at 500 hPa and water vapor flux with its divergence at 850 hPa. The daily global precipitation analysis (spatial resolution: 0.5° × 0.5°) from the Climate Prediction Center (CPC) was used to evaluate the WRF model precipitation simulation performance. CPC precipitation data applies an optimal interpolation technique to convert precipitation reports from roughly 16,000 stations over the global land areas to a grid (Chen et al. 2008).

The simulation performance was quantitatively assessed using root-mean-square error (RMSE). The RMSE is defined as follows:

$$RMSE = \sqrt{\frac{1}{n}\sum_{i=1}^{n}\left(F_i - O_i\right)^2} \quad (1)$$

where F and O are the simulation and verifying observation with the same physical units and N is the total grid points in the validation domain.

2.2 Definition of SFTZ

The SFTZ is a region that is surrounded by 0 °C isotherms in January and by an annual climatological mean of 0 °C isotherms (Zhang et al. 2003; Jiang and Wang 2020). The SFTZ in this study is shown in Fig. 1, circled with a blue line. Figure 1 further shows that the maximum standard deviation of spring SM at soil depth 0–1 m from ERA5 occurs primarily over the SFTZ in the mid-latitudes of the NH, indicating that the largest inter-annual variability of SM is in the SFTZ (Yang et al. 2016).

2.3 Experimental design

To exclude the impacts from sea surface temperature anomalies, a 7-month simulation (February–August 2004) based on the WRF model (version 3.9.1) was conducted because neither an El Niño nor a La Niña event occurred in 2004. Figure 1 shows the simulation domain, which covers the entire NH with 360 × 360 grid points. The selected physical parameterization schemes for the simulation were the Kain–Fritsch cumulus scheme (Kain 2004), the Rapid Radiative Transfer Model for General Circulation Models (RRTMG, Iacono et al. 2008) for the longwave and shortwave radiation schemes, the ACM2 (Pleim) planetary boundary layer scheme (Pleim 2007), the Pleim-Xiu surface layer scheme (Pleim 2006), the WRF Double-Moment 6-Class cloud microphysics scheme (Lim and Hong 2010), and the Pleim–Xiu land surface scheme (Pleim and Xiu 2003). The Pleim–Xiu land surface scheme contains a surface soil layer (0–1 cm) and a deep soil layer (1–100 cm).

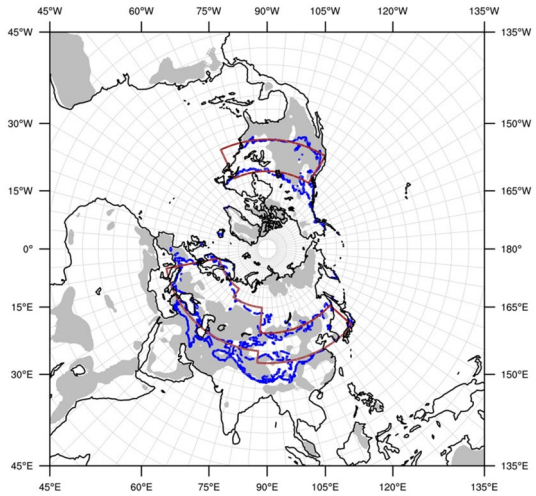

Fig. 1 Simulation domain in this study. Regions surrounded by blue lines indicate the seasonal frozen-thawing zone (SFTZ, dashed and solid isotherms lines represent January 0 °C and annual 0 °C, separately, on climatological mean). Brown lines denote the region where soil moisture (SM) is assimilated. Gray shaded colors indicate regions where the standard deviation of spring (March–May average) SM at 1-m depth are larger than 0.025 m^3 m^{-3} for the period 1979–2019 from ERA5

Two experiments were designed to investigate the effects on subsequent summer precipitation in the NH from correcting spring SM biases over the SFTZ: the control experiment (CTL), which used the Pleim–Xiu land surface scheme (Pleim and Xiu 2003) without assimilating any observations, and the assimilation experiment (ISN), which used the ISN method in the Pleim–Xiu land surface scheme to assimilate spring SM in the SFTZ.

In the ISN experiment, SM tendencies were updated every 3 h by comparing the current forecast values of T_{2m} and RH_{2m} with the observed values interpolated from periodic objective analyses. The technique of nudging soil moisture tendency is adopted by Pleim and Xiu (2003).

$$\frac{\partial w_g}{\partial t} = \alpha_1\left(T^a - T^f\right) + \alpha_2\left(RH^a - RH^f\right) \quad (2)$$

$$\frac{\partial w_2}{\partial t} = \beta_1\left(T^a - T^f\right) + \beta_2\left(RH^a - RH^f\right) \quad (3)$$

where w_g is the SM in surface soil layer; w_2 is the SM in deep soil layer; t is the time; T^a is observed values of T_{2m}; T^f is the current forecast values of T_{2m}; RH^a is observed values of RH_{2m}; RH^f is the current forecast values of RH_{2m};α_1,α_2 ,β_1 and β_2 is the nudging coefficients are computed from relevant model parameters in model time step which reflect the coupling between the soil layers and the near-surface atmospheric layer. Therefore, soil moisture is dynamically adjusted according to model biases of T_{2m} and RH_{2m} and nudging strengths computed from model parameters. During the night in the spring in the ISN experiment, deep temperature nudging was used to complement SM nudging according to the model bias in T_{2m} because surface forcing is weak at that time (Pleim and Gilliam 2009).

3 Improvement of the SM simulation in the SFTZ by assimilating spring SM

To investigate the effectiveness of spring SM assimilation in the SFTZ on correcting SM simulation biases, the correlation coefficients of SM between two experiment (CTL and ISN) simulations and three reanalysis datasets (ERA-Interim, ERA5, and GLDAS2.1 Noah) are shown in Fig. 2. In the CTL experiment, SM shows no significant correlation with ERA-Interim, ERA5, or GLDAS2.1 Noah across the mid-latitudes (Fig. 2a–c). This suggests that spring SM variations in the SFTZ are not captured in the CTL experiment, which implies that the spring soil thawing processes are poorly represented. After assimilating spring SM in the SFTZ, significant correlations reveal that SM in the ISN experiment is consistent with the three reanalysis datasets in the SFTZ (Fig. 2d–f). A noteworthy feature is that in either CTL or ISN experiment, SM has high correlation between simulation and three reanalysis datasets outside SFTZ, especially in high and lower latitude regions (Fig. 2a–f). It illustrates that there are same SM variability and tendency between model ICBC and reanalysis data in these regions, and correcting spring SM biases in SFTZ couldn't change this relation in ISN experiment.

To further investigate the effects of assimilating spring SM in the SFTZ on SM simulations, the differences in SM between two experiments (CTL and ISN) and three reanalysis data (ERA-Interim, ERA5, and GLDAS2.1 Noah) were calculated (Fig. 3). Previous studies (e.g., Douville et al. 2001; Yang et al. 2016) suggested that SM impacts precipitation more than oceanic effects in mid-latitudes, and to analyze the performance of SM assimilation, SM variation in the North America and Eurasia at the 30–60° N was selected to represent SM variation in the SFTZ because the SFTZ is essentially located in this region, though the boundary of the SFTZ shows inter-annual variations. It was evident that there are wet biases of SM simulation in the two experiments in the SFTZ and in the NH (Fig. 3a–c). The wet biases of SM in the CTL experiment have no consistent increasing or decreasing trend in the North American SFTZ

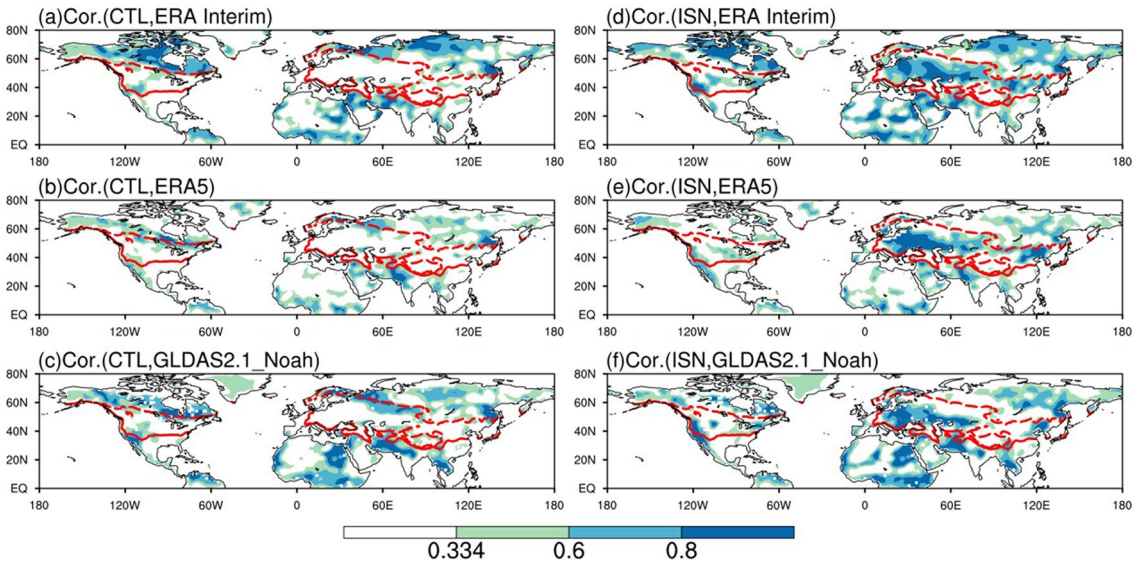

Fig. 2 Correlation coefficients of spring SM (unit: $m^3\ m^{-3}$) at 1-m depth between the CTL experiment and **a** ERA-Interim, **b** ERA5, **c** GLDAS2.1 Noah. **d–f** Same as **a–c** but for the ISN experiment. The shaded areas (correlation coefficients > 0.334) proved statistically significant at the 99.9% confidence level. Regions surrounded by red lines are the SFTZ

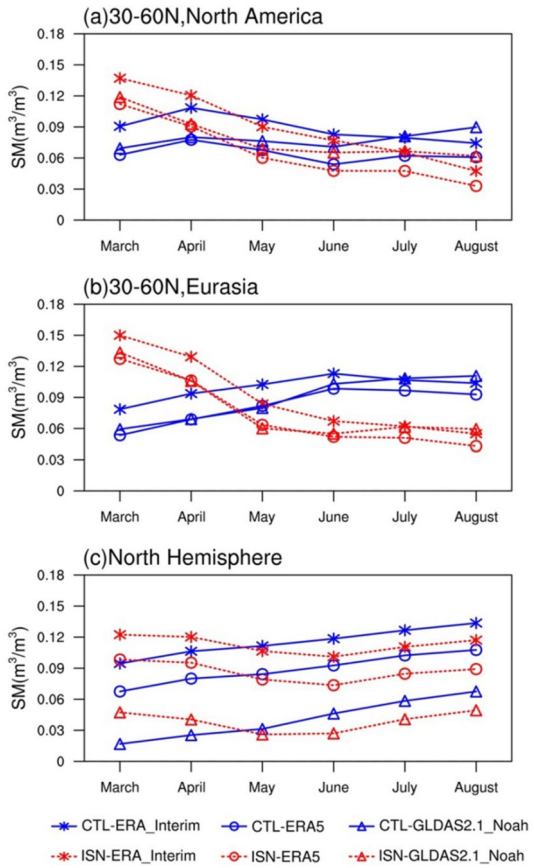

Fig. 3 The difference of area-averaged SM between experiments (CTL and ISN) and reanalysis data (ERA-Interim, ERA5, and GLDAS2.1 Noah) over **a** North America at 30–60° N, **b** Eurasia at 30–60° N, and **c** Northern Hemisphere

(Fig. 3a), an increasing trend from March to June in the Eurasian SFTZ (Fig. 3b), and an increasing trend overall in the NH (Fig. 3c). After assimilating spring SM in the SFTZ, wet biases of SM in the SFTZ had a clearly descending trend from March to August in the ISN experiment (Fig. 3a, b). In the NH (Fig. 3c), wet biases of SM in the ISN experiment decreased from March to June and increased from June to August. This suggests that assimilating spring SM in the SFTZ cannot suppress the overall increasing wet biases of SM in the NH from June to August. In addition, wet biases of SM in the ISN experiment are smaller than those in the CTL experiment from May to August. As shown in Figure 3, there are large increases of SM wet biases from March to April in the CTL experiment, which means that SM variation from March to April cannot be well simulated. This may be because soil is still frozen. In the CTL experiment, it was found that SM wet biases in the SFTZ only had a slight variation from June to August when compared with the variation from March to June (Fig. 3a, b), and wet SM biases in the NH maintain a consistent increasing trend from March to August (Fig. 3c). This suggests that the wet biases of SM in the SFTZ are primarily induced in the spring, and the wet biases of SM in May influence the degree of wet biases of SM in the summer in the SFTZ, whereas wet biases of SM outside the SFTZ still increase in the summer. This reflects the importance of the assimilation of spring SM in the SFTZ on the subsequent summer climate prediction. Additionally, it is found that the wet biases of SM decrease the most from April to May in the ISN experiment (Fig. 3a–c), which suggests that the assimilation of spring SM in the SFTZ may be more suitable from April to May than in March.

As the wet biases of SM in the SFTZ in May approximately reflect the wet biases of SM in the summer and influence the subsequent climate in June and July due to SM memory, the biases of SM in May are calculated in Fig. 4. The main biases of SM in the CTL experiment in May are more concentrated in the SFTZ when compared with the three reanalysis data (Fig. 4a–c). Results in Fig. 4d–f suggest that assimilating spring SM in the SFTZ decreases the wet biases of SM in May in the ISN experiment on the whole. The wet SM biases in few regions seem to have a little increase which might be due to the biases in the assimilated observations in these regions, that need to further investigate.

Overall, the simulation biases of SM in the SFTZ are clearly reduced in the ISN experiment compared to the CTL experiment. In the next section, the effects of the correcting SM simulation biases in the SFTZ on subsequent summer precipitation simulations over the NH will be analyzed.

4 Effects of correcting spring SM simulation biases in the SFTZ on the subsequent summer precipitation simulation in the NH

To evaluate the simulation performance of summer precipitation after correcting spring SM simulation biases in the SFTZ, the RMSE of land precipitation was calculated based on CPC precipitation data, while the RMSEs of three latitude bands of precipitation were calculated to assess if correcting spring SM biases in the SFTZ improved the subsequent summer precipitation simulation in the NH (Fig. 5).

In the low and middle latitudes (Fig. 5a, b), RMSEs of summer precipitation in June, July, and the overall summer simulated by ISN are lower than that in CTL, whereas a higher RMSE is found in August in the ISN experiment. This indicates that correcting spring SM biases in the SFTZ improves land precipitation simulations in summer (primarily caused by improvements in June, July) in the lower and middle latitudes. Similarly, land precipitation simulation in June, August become poor in the high latitudes which lead to poor simulation of summer precipitation in the high latitudes (Fig. 5c). Considering the Fig. 4, poor

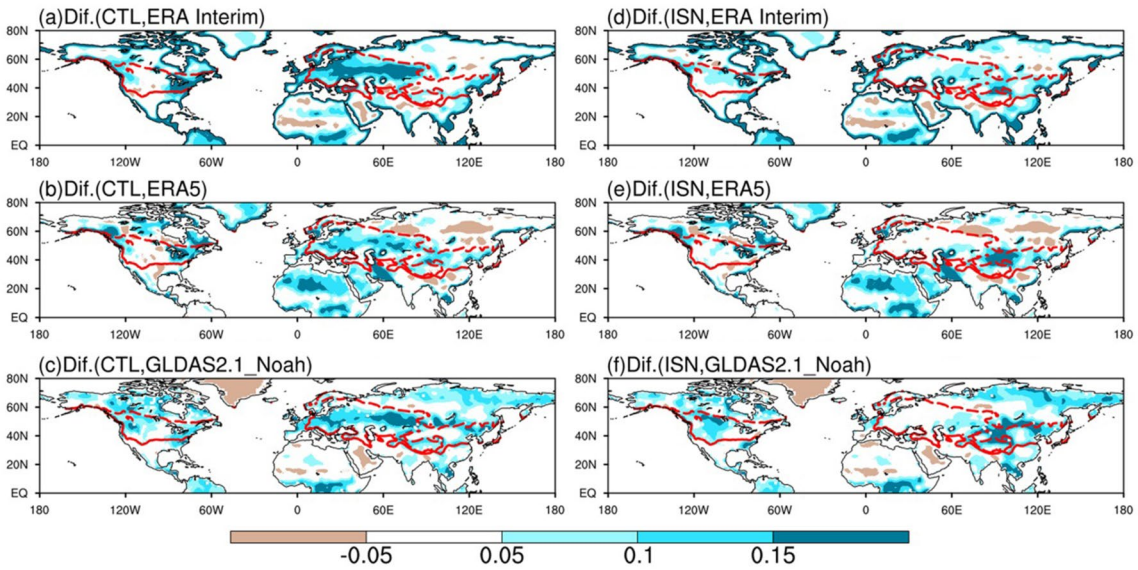

Fig. 4 The difference of SM (unit: $m^3\ m^{-3}$) at 1-m depth in May between the CTL experiment and **a** ERA-Interim, **b** ERA5, and **c** GLDAS2.1 Noah. **d–f** Same as **a–c** but for the ISN experiment. Regions surrounded by red lines are the SFTZ

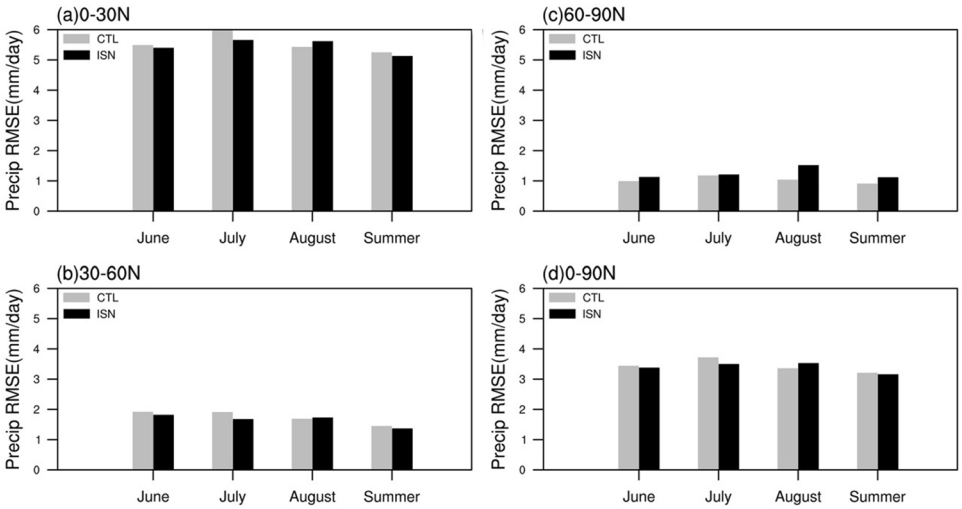

Fig. 5 Root-mean-square error (RMSE) of land precipitation (unit: mm day^{-1}) in June, July, August, and the general summer at **a** 0–30° N, **b** 30–60° N, **c** 60–90° N, and **d** 0–90° N in comparison with the precipitation from CPC. The gray (black) bars indicate the RMSE of the CTL (ISN) experiment

precipitation simulation can be interpreted by SM biases exist in high latitudes in both model ICBC and reanalysis datasets, although SM has same tendency in high latitudes in Fig. 2. The simulation performance of land precipitation in the NH (Fig. 5d) is similar to the results in the low and middle latitudes (Fig. 5a, b). Therefore, correcting spring SM biases in the SFTZ can influence summer precipitation prediction in the NH. In addition, the improvement of land precipitation simulation in summer in the NH is located in the low and middle latitudes in June and July.

To investigate the reasons for the differences in simulation performance of land precipitation in the two experiments, the ratio of precipitation biases of the CTL experiment and the ISN experiment is calculated based on CPC precipitation data (Fig. 6). The ratio in Fig. 6a–d was calculated by dividing precipitation biases of the CTL experiment by precipitation biases of the ISN experiment, where absolute value greater than 1 for the ratios indicate that the ISN experiment has a better precipitation simulation. The ratios in Fig. 6e–h are the multiplicative inverse of results in Fig. 6a–d which means that the CTL experiment has a better precipitation simulation with absolute values of a ratio greater than 1.0. There are basically wet biases of precipitation in the CTL and ISN experiments (figures not shown). Therefore, the results shown in Fig. 6a–c suggest that correcting spring SM biases in the SFTZ improved the summer precipitation simulation by decreasing the wet biases of precipitation. However, the results in Fig. 6e–h show that correcting SM biases

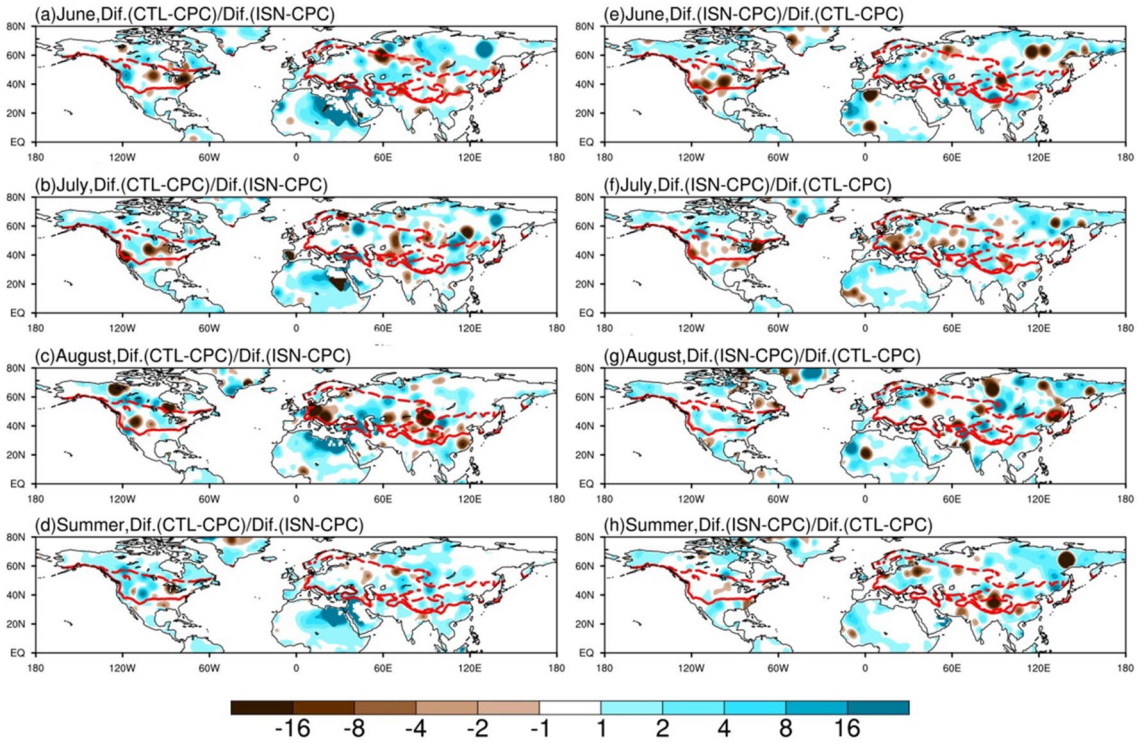

Fig. 6 Left panel: the ratio between the precipitation biases of the CTL experiment (CTL minus CPC) and the ISN experiment (ISN minus CPC) in **a** June, **b** July, **c** August, and **d** summer. Right panel: the multiplicative inverse of ratio in the left panel in **e** June, **f** July, **g** August, and **h** summer. Absolute values of a ratio greater than 1 in the left (right) panel indicate that the ISN (CTL) experiment has better performance of precipitation simulation than has the CTL (ISN) experiment. Regions surrounded by red lines are the SFTZ

also cause a worse precipitation simulation by increasing the wet biases of precipitation.

Correcting wet biases in spring SM in the SFTZ can significantly improve the land precipitation simulation in June and July in the low and middle latitudes. Precipitation simulation in August is not improved, especially in the high latitudes. Overall, the summer precipitation simulation is improved in the NH.

5 Improvement of elements in land–atmosphere interaction after correcting SM biases in the SFTZ

Section 4 provided evidence that correcting spring SM biases in the SFTZ can improve the summer precipitation simulation. Because SM is important for regulating land–atmosphere interactions, the differences in the precipitation simulations of the two experiments should be related to the land–atmosphere interactions affected by SM changes. Thus, the next question that needs to be further investigated is: what changes in quantities of land–atmosphere interactions occur after assimilation?

To investigate the surface heat changes caused by correcting spring SM biases in the SFTZ, the RMSE of LH and SH at 30–60°N of the two experiments (CTL and ISN) is compared with the three reanalysis data (ERA-Interim, ERA5, and GLDAS2.1 Noah), as shown in Fig. 7. Similar to the comparison of SM variation (Fig. 3), LH and SH at 30–60°N are selected. Results show that ISN experiment has a worse LH simulation from March to June compared with the three reanalysis data, but the ISN experiment has a better LH simulation from July to August compared with ERA-Interim, and ERA5 and a worse LH simulation from July to August compared with GLDAS2.1 Noah (Fig. 7a–c). Overall, the ISN experiment has a worse LH simulation in the spring and a better LH simulation in the summer compared with the CTL experiment. The ISN experiment has a better SH simulation from April to July, but it is difficult to judge which experiment has a better SH simulation in March and August when compared with the three reanalysis data (Fig. 7d–f). Overall, the ISN experiment has a better SH simulation in the spring and summer. These results indicate that correcting spring SM biases in the SFTZ improve the SH simulation in the SFTZ in the spring and summer, but the improvement of LH simulation in the spring is marginal.

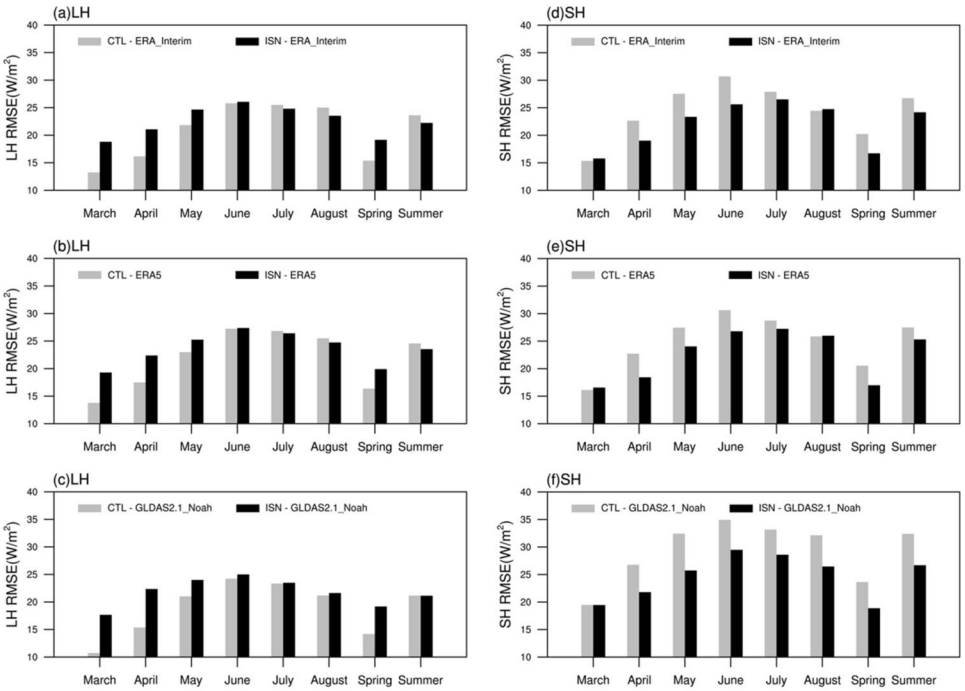

Fig. 7 RMSE of land surface latent heat flux (LH, unit: W m^{-2}) compared with **a** ERA-Interim, **b** ERA5, and **c** GLDAS2.1 Noah at 30–60° N from March to August and in the spring and summer. **d–f** Same as **a–c** but for sensible heat flux (SH, unit: W m^{-2}). The gray (black) bars indicate the RMSE of the CTL (ISN) experiment

To investigate why correcting spring SM biases in the SFTZ changes the LH and SH simulations in the SFTZ, the simulation biases of spring and summer LH in the two experiments (CTL and ISN) were compared with the three reanalysis data (ERA-Interim, ERA5, and GLDAS2.1 Noah), as shown in Figs. 8, 9, 10, 11. It can be seen that the spatial pattern of biases of SH and LH outside of the SFTZ is similar between the two experiments. In Figs. 8, both experiments exhibit positive biases for LH in the SFTZ in spring, with the biases being relatively smaller for the CTL experiment. In summer, both positive and negative biases of LH can be found in the SFTZ in the two experiments (Figs. 9). It is evident that LH biases of the CTL experiment increased from spring to summer, which led to a larger LH RMSE in the CTL experiment than that in the ISN experiment in the summer (Fig. 7a–c).

For SH, the CTL experiment has negative SH biases in spring in the SFTZ while the ISN experiment had smaller

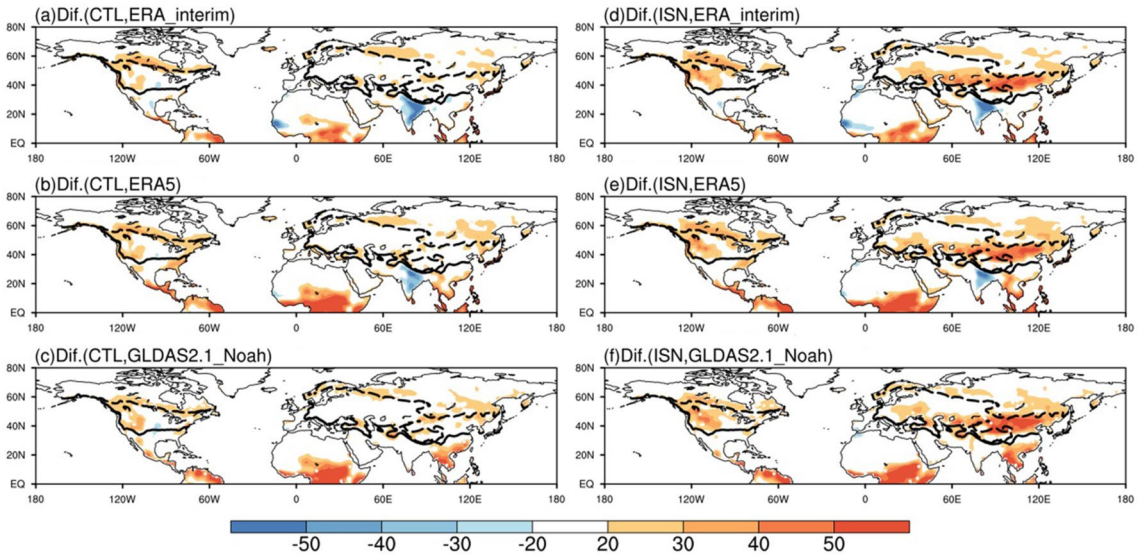

Fig. 8 Differences in spring LH (unit: W m^{-2}) between the CTL experiment and **a** ERA-Interim, **b** ERA5, and **c** GLDAS2.1 Noah. **d–f** Same as **a–c** but for the ISN experiment. Regions surrounded by black lines are the SFTZ

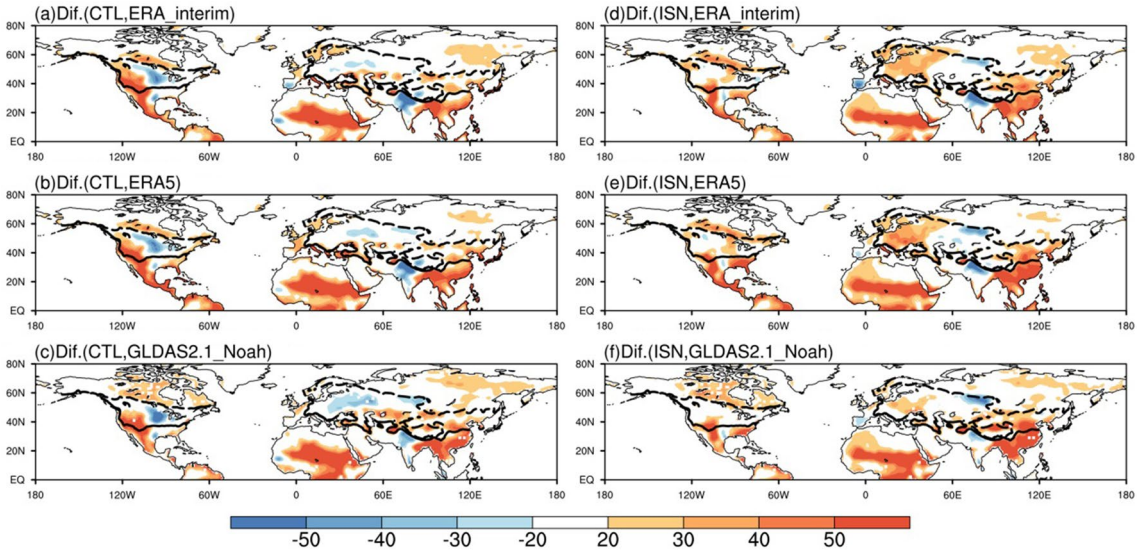

Fig. 9 Differences in summer LH (unit: W m^{-2}) between the CTL experiment and **a** ERA-Interim, **b** ERA5, and **c** GLDAS2.1 Noah. **d**–**f** Same as **a**–**c** but for the ISN experiment. Regions surrounded by black lines are the SFTZ

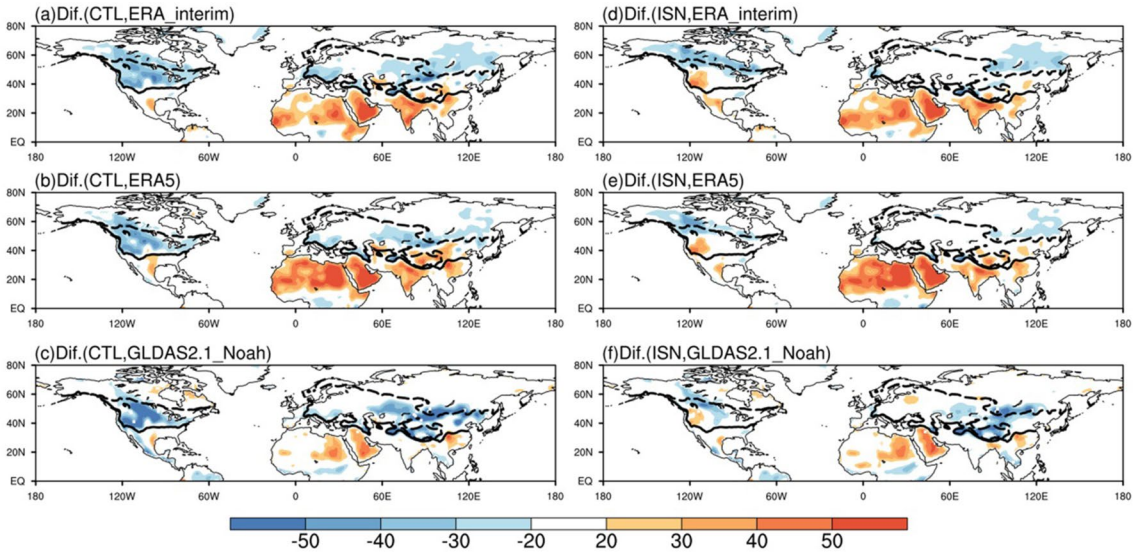

Fig. 10 Differences in spring SH (unit: W m^{-2}) between the CTL experiment and **a** ERA-Interim, **b** ERA5, and **c** GLDAS2.1 Noah. **d**–**f** Same as **a**–**c** but for the ISN experiment. Regions surrounded by black lines are the SFTZ

SH biases in spring in the SFTZ (Fig. 10). Consequently, SH biases in the SFTZ in the CTL experiment clearly increased in the summer (Fig. 11a–c), whereas the ISN experiment only has positive SH biases in the summer around central Asia (Fig. 11d–f). These results explain the smaller RMSE of SH in the SFTZ in the ISN experiment from spring to summer (Fig. 7d–f).

The spatial pattern of evapotranspiration biases is similar to the LH biases pattern in the two experiments (Figures not shown). After correcting spring SM biases in the SFTZ, the simulation of evapotranspiration was adjusted, which subsequently influenced the simulation of LH and SH. Overall, correcting spring SM biases in the SFTZ improved the simulation of summer LH and spring and summer SH in the SFTZ. Specifically, it suppressed the increase of LH biases in the SFTZ in summer, though assimilating spring SM in the SFTZ caused the worse simulation of evaporation in spring. Additionally, correcting spring SM biases in the SFTZ also continuously corrects the cold SH biases from spring to summer. Therefore, correcting spring SM biases in the SFTZ indeed improved the land surface energy conditions in the SFTZ,

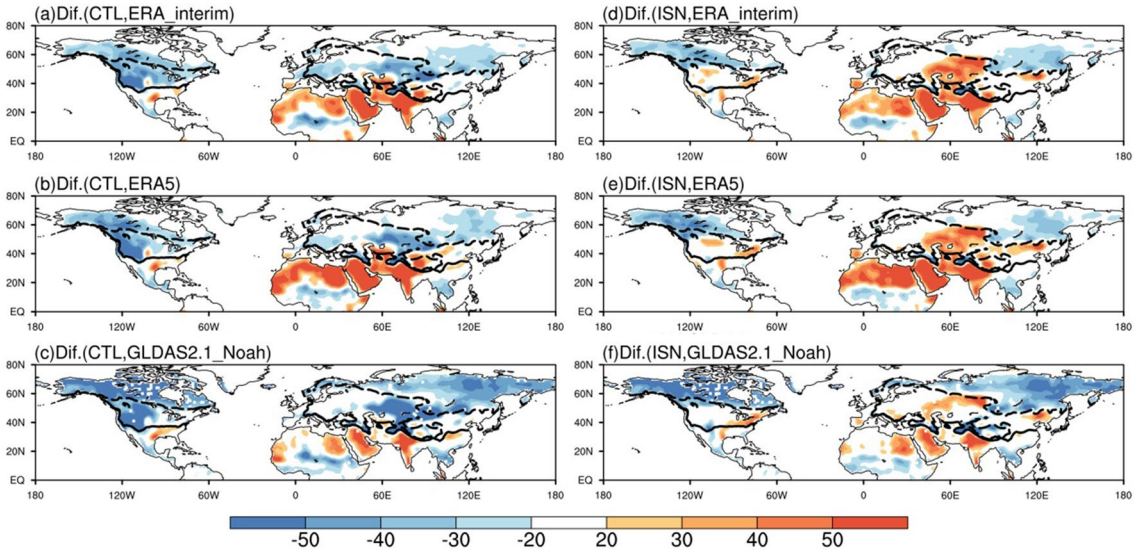

Fig. 11 Differences in summer SH (unit: W m^{-2}) between the CTL experiment and **a** ERA-Interim, **b** ERA5, and **c** GLDAS2.1 Noah. **d**–**f** Same as **a**–**c** but for the ISN experiment. Regions surrounded by black lines are the SFTZ

which are beneficial to the summer precipitation simulation in the NH.

6 Possible mechanisms for the contribution of correcting spring SM biases in the SFTZ to the subsequent summer precipitation

As demonstrated by Yang et al. (2016), energy anomalies on the land surface of the SFTZ can induce anomalous circulations, which subsequently influence the summer precipitation simulation.

To assess the atmosphere circulation simulation, RMSEs of the 500-hPa geopotential height are calculated for spring and summer from March to August (Fig. 12). There were smaller RMSEs of the 500-hPa geopotential height in the low latitudes (Fig. 12a) than in the middle and high latitudes (Fig. 12b, c). The biases of the ISN experiment are similar to those in the CTL experiment because the atmospheric circulations in the low latitudes are dominated by tropical sea surface temperature. In the mid-latitudes, the ISN experiment has a better simulation of the 500-hPa geopotential height than the CTL experiment, except for that in April (Fig. 12b). In the high latitudes, the ISN experiment has a better simulation of the 500-hPa geopotential height than that in the CTL experiment, except for that in March and August (Fig. 12c). Similarly, in the NH, the ISN experiment has a better simulation of the 500-hPa geopotential height than has the CTL experiment, except for that in March and August (Fig. 12d). The worse simulations of 500-hPa geopotential height in the NH in March and August are primarily due to the worse simulation in the high latitudes. The simulation of the 500-hPa

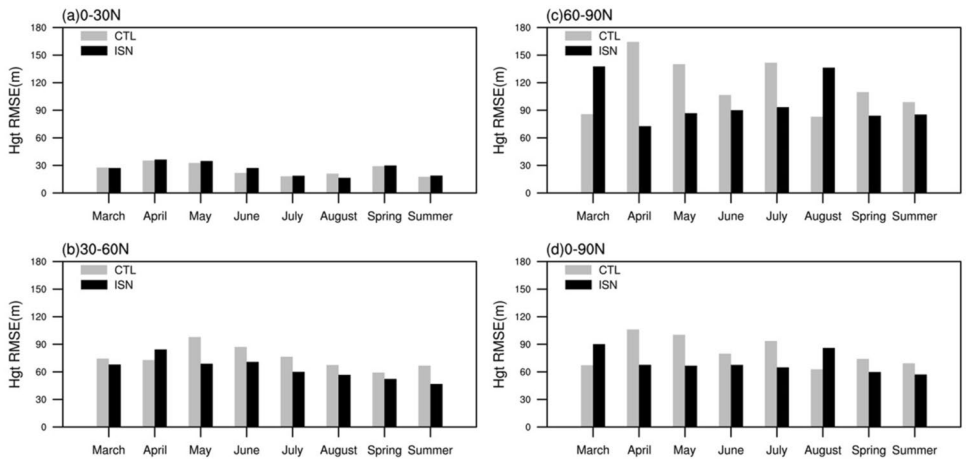

Fig. 12 RMSE of the 500-hPa geopotential height (unit: m) at **a** 0–30° N, **b** 30–60° N, **c** 60–90° N, and **d** 0–90° N from March to August and in the spring and summer compared with ERA5. The gray (black) bars indicate the RMSE of the CTL (ISN) experiment

geopotential height is clearly improved in the middle and high latitudes in June and July (Fig. 12b, c), which may be responsible for the improvement of the precipitation simulation in the low and middle latitudes in June and July.

To further investigate the reasons for the improvement of the 500-hPa geopotential height, simulation biases of the 500-hPa geopotential height in two experiments (CTL and ISN) were compared with that in ERA5, as shown in Fig. 13. There are mostly negative biases of the 500-hPa geopotential height in the CTL experiment from June to August, as well as in the whole summer, and the positive biases are mainly located over the ocean (Fig. 13a–d). By correcting spring SM biases in the SFTZ, the negative biases of the 500-hPa geopotential height in June and July are reduced on the whole, but it also causes an increase of positive biases of the 500-hPa geopotential height (Fig. 13e, f), especially over the northern Europe in June. Correcting spring SM biases in the SFTZ also leads to an increase in the negative biases of the 500-hPa geopotential height around northwestern North America in August (Fig. 13g), which explains the larger biases of the 500-hPa geopotential height in the ISN experiment than those in the CTL experiment in the high latitudes (Fig. 12c). In addition, negative biases of the 500-hPa geopotential height in high latitudes in the ISN experiment (Fig. 13e, f, and h) may be caused by the SM biases in high latitudes in Fig. 4 which explain the deterioration of precipitation simulation the high latitudes (Fig. 5c) in the ISN experiment. Overall, assimilating spring SM in the SFTZ improves the 500-hPa geopotential height in the summer in the NH (Fig. 13h).

As the water vapor condition in the lower atmosphere is essential for precipitation, the water vapor flux (WVF) and its divergence at 850 hPa in the summer is compared between two experiments (CTL and ISN) and ERA5 (Fig. 14). By comparing the biases of the CTL and ISN

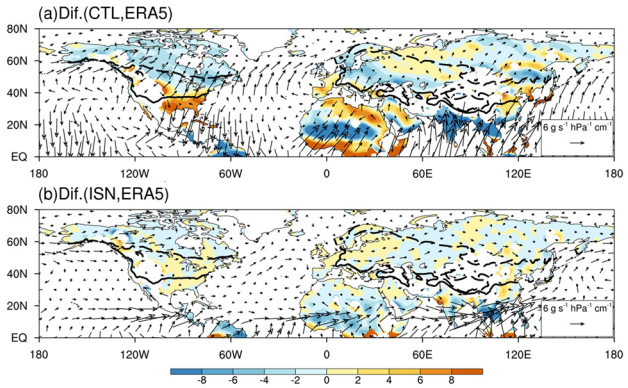

Fig. 14 The difference in water vapor flux (vector, g s^{-1} hPa^{-1} cm^{-1}) and its divergence (shading, 10^{-6} g s^{-1} hPa^{-1} cm^{-2}) at 850 hPa in the summer between **a** the CTL experiment and ERA5, and **b** the ISN experiment and ERA5. Regions surrounded by black lines are the SFTZ

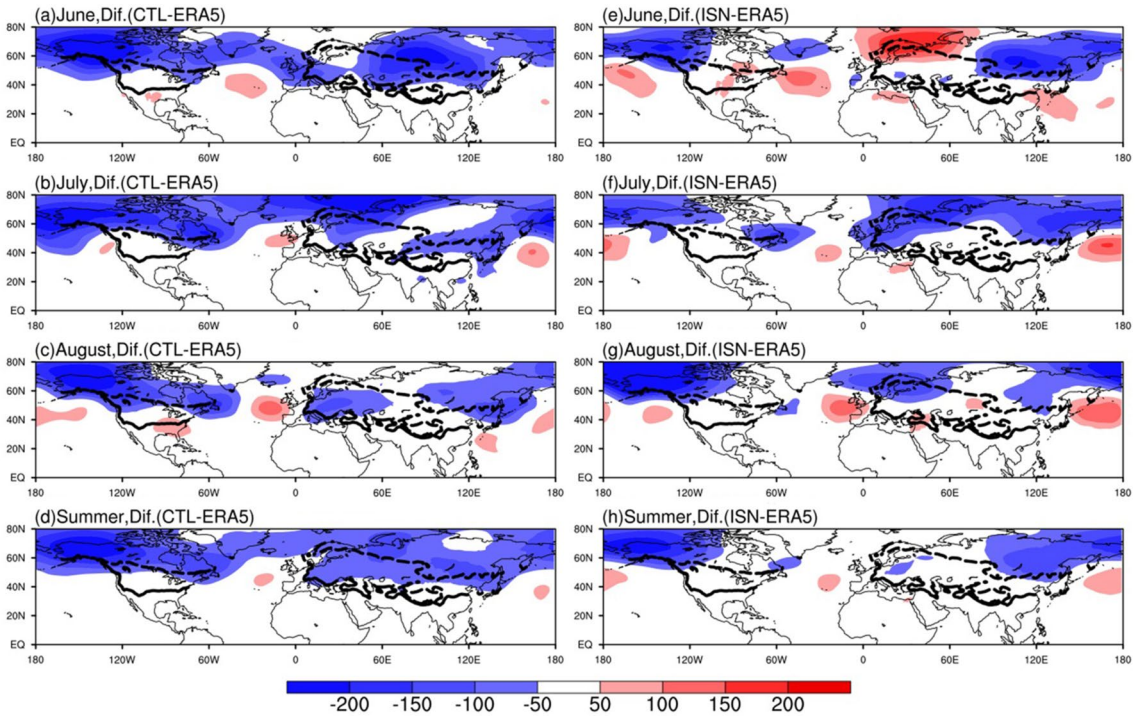

Fig. 13 Differences in the 500-hPa geopotential height (unit: m) between the CTL experiment and ERA5 in **a** June, **b** July, **c** August, and **d** summer. **d**–**f** Same as **a**–**c** but for the ISN experiment. Regions surrounded by black lines are the SFTZ

experiments, it is evident that larger WVF biases of the CTL experiment are found in the NH than those of the ISN experiment. Subsequently, stronger WVF convergence biases are found in the CTL experiment than those in the ISN experiment. These results are responsible for the decrease in wet biases of precipitation shown in Fig. 6.

Overall, correcting spring SM biases in the SFTZ improves the subsequent summer precipitation simulation by improving the simulation of large-scale circulation and water vapor conditions in the NH during the summer.

7 Conclusions

This study investigated the impacts of correcting SM biases in the SFTZ over the NH on the subsequent summer precipitation simulation, using the ISN method in the WRF model. The results suggest that correcting biases of spring SM in the SFTZ can improve the land–atmosphere interaction processes in the spring and summer. In other words, the SFTZ is a crucial region (hot spot) for land–atmosphere interaction.

After correcting spring SM biases in the SFTZ, the simulated variations of SM in the SFTZ from the ISN experiment were significantly correlated with SM from the three reanalysis data (ERA-Interim, ERA5, and GLDAS 2.1 Noah), whereas SM from the CTL experiment showed no significant correlation. Additionally, SM outside of the SFTZ in the two experiments are consistent with SM from the three reanalysis data during the spring, further indicating that the SFTZ is a key region for general circulation anomalies in spring. Assimilating spring SM in the SFTZ also reduces wet biases of SM, causing the SM in the ISN experiment to be closer to the SM in the three reanalysis data in the SFTZ from May to August. Furthermore, wet SM biases are not significantly increased after May in the SFTZ, which suggests that SM biases in May could dominate the magnitude of SM biases in the summer. These results indicate that correcting spring SM biases in the SFTZ can represent the variations of SM during the summer and would improve precipitation simulation in the summer.

The precipitation simulation results show that the ISN experiment has a better performance in the low and middle latitudes in June and July. Wet biases of precipitation are more dominant than dry biases in both the CTL and ISN experiments. Assimilating spring SM in the SFTZ decreases the wet biases of summer precipitation. This explains that correcting the spring SM biases in the SFTZ can reduce the negative biases of SH in the CTL experiment during spring and summer and it can also decrease the biases of LH in summer. In other words, by assimilating spring SM in the SFTZ, correcting SM can provide a better expression of land surface energy in the SFTZ in the summer.

Correcting spring SM biases in the SFTZ produces a positive effect on precipitation simulations, which is attributed to the improved simulation of the 500-hPa geopotential height in the middle and high latitudes in June and July. However, because persistence effect of SM on atmosphere is approximately 120 days (Yang and Wang 2019b), the simulation performance becomes worse in August. Further investigation suggests that spring SM improvements in the SFTZ can decrease negative biases of the 500-hPa geopotential height in the middle and high latitudes in June and July, while it increases the negative biases in the middle and high latitudes in August. Similarly, correcting spring SM biases in the SFTZ can clearly decrease the WVF and WVF convergence biases. These results demonstrated that spring SM in the SFTZ affects precipitation production and relative general circulation and water vapor conditions throughout the NH in the summer, especially in June and July.

This study provides the evidence that improving spring SM variability in the SFTZ over the NH can improve the subsequent summer precipitation simulations. However, the improvement of summer precipitation mainly locates in low and middle latitudes in June and July, while precipitation simulations become a little bit worse in August in high latitudes. On one hand, it might attribute to that the SM biases in high latitudes. On the other hand, the SM variability caused by snow melting in high latitudes is not considered. In addition, the SM in spring should be assimilated according to the soil frozen-thawing state in the ISN scheme to achieve better simulation results. The frozen-thawing processes of soil in spring are not well simulated by numerical models which cause the significant model biases (Yang and Wang 2018; Yang et al. 2018). The ISN scheme should be developed and optimized for soil frozen-thawing processes. These are worthy to be further investigated. This work shows that the land–atmosphere interaction over the SFTZ in spring has crucial impact on general circulation anomaly in the NH and can influence the subsequent summer precipitation in the NH.

Acknowledgements This study is supported by the National Natural Science Foundation of China (NSFC, Nos. 42175064, 91837205, 41805032 and 41975111), and Science Foundation of Gansu province in China (20JR10RA654). We appreciate the European Centre for Medium Range Weather Forecasts (ECMWF) for providing the ERA-Interim reanalysis data (http://apps.ecmwf.int/datasets/data/interim-full-moda/levtype=sfc/) and ERA5 reanalysis data (https://cds.climate.copernicus.eu/cdsapp#!/dataset/reanalysis-era5-pressure-levels?tab=form), the National Centers for Environmental Prediction (NCEP) for providing the NCEP Automated Data Processing (ADP) global surface observational weather data (https://rda.ucar.edu/datasets/ds461.0/) and final analysis data (FNL, http://rda.ucar.edu/datasets/ds083.2), the National Aeronautics and Space Administration (NASA) Goddard Space Flight Center (GSFC) Hydrological Sciences Laboratory (HSL) and the Goddard Earth Sciences Data and Information Services Center (GES DISC) for providing Global Land Data Assimilation System Version 2 (GLDAS-2) data (https://disc.gsfc.nasa.gov/datasets), and the

National Oceanic and Atmospheric Administration (NOAA) Climate Prediction Center for providing daily global precipitation data (https://psl.noaa.gov/data/gridded/data.unified.daily.conus.html).

References

Amenu GG, Kumar P, Liang XZ (2005) Interannual variability of deep-layer hydrologic memory and mechanisms of its influence on surface energy fluxes. J Clim 18(23):5024–5045

Bounoua L, Krishnamurti TN (1993) Influence of soilmoisture on the Sahelian climate prediction I. Meteorol Atmos Phys 52:183–203

Chen F, Mitchell K, Schaake J, Xue Y, Pan HL, Koren V, Duan QY, Ek M, Betts A (1996) Modeling of land-surface evaporation by four schemes and comparison with FIFE observations. J Geophys Res 101(D3):7251–7268. https://doi.org/10.1029/95JD02165

Chen M, Wei S, Xie P, Silva V, Kousky VE, Higgins RW, Janowiak JE (2008) Assessing objective techniques for gauge-based analyses of global daily precipitation. J Geophys Res Atmos 113(D4)

Decker M, Brunke MA, Wang Z, Sakaguchi K, Zeng X, Bosilovich MG (2012) Evaluation of the reanalysis products from GSFC, NCEP, and ECMWF using flux tower observations. J Clim 25(6):1916–1944. https://doi.org/10.1175/JCLI-D-11-00004.1

Dee DP, Uppala SM, Simmons AJ, Berrisford P, Poli P, Kobayashi S, Andrae U, Balmaseda MA, Balsamo G, Bauer DP, Bechtold P (2011) The ERA-Interim reanalysis: configuration and performance of the data assimilation system. Q J R Meteorol Soc 137(656):553–597

Dirmeyer PA (2011) History and review of the global soil wetness project (GSWP). J Hydrometeorol 12(5):729–749

Douville H (2002) Influence of soil moisture on the Asian and African monsoons Part II: interannual variability. J Clim 15:701–720

Douville H (2009) Relative contribution of soil moisture and snow mass to seasonal climate predictability: a pilot study. Clim Dyn 34:797–818. https://doi.org/10.1007/s00382-008-0508-1

Douville H, Chauvin F, Broqua H (2001) Influence of soil moisture on the Asian and African monsoons. Part I: mean monsoon and daily precipitation. J Clim 14:2381–2403

Ferguson CR, Wood EF, Vinukollu RK (2012a) A global intercomparison of modeled and observed land-atmosphere coupling. J Hydrometeorol 13(3):749–784. https://doi.org/10.1175/JHM-D-11-0119.1

Ferguson CR, Wood EF, Vinukollu RK (2012b) A global intercomparison of modeled and observed land–atmosphere coupling. J Hydrometeorol 13(3):749–784

Gao H, Wood EF, Drusch M, Jackson T, Bindlish R (2006) Using TRMM/TMI to retrieve soil moisture over the southern United States from 1988 to 2002. J Hydrometeorol 7:23–38

Guo Z, Dirmeyer PA (2006) Evaluation of the second global soil wetness project soil moisture simulations: 1. Intermodel comparison. J Geophys Res Atmos 111(D22):1–14

Hersbach H, Bell B, Berrisford P, Hirahara S, Horányi A, Muñoz-Sabater J et al (2020) The ERA5 global reanalysis. Q J R Meteorol Soc 146(730):1999–2049. https://doi.org/10.1002/qj.3803

Iacono MJ, Delamere JS, Mlawer EJ, Shephard MW, Collins WD (2008) Radiative forcing by long–lived greenhouse gases: calculations with the AER radiative transfer models. J Geophys Res 113:D13103

Jiang JH, Wang CH (2020) Study on the relationship between seasonal freezing-thawing areas and summer precipitation in the Northern Hemisphere. J Glaciol Geocryol 42(1):53–61

Kain JS (2004) The Kain-Fritsch convective parameterization: an update. J Appl Meteorol 43(1):170–181

Kerr YH, Waldteufel P, Richaume P, Wigneron JP (2012) The SMOS soil moisture retrieval algorithm. IEEE Trans Geosci Remote Sens 50(5):1384–1403

Koren V, Schaake J, Mitchell K, Duan QY, Chen F (1999) A parameterization of snowpack and frozen ground intended for NCEP weather and climate models. J Geophys Res 104(D16):19569–19585. https://doi.org/10.1029/1999JD900232

Koster RD, Dirmeyer PA, Guo ZC et al (2004) Regions of strong coupling between soil moisture and precipitation. Science 305(5687):1138–1140

Koster RD, Mahanama SPP, Yamada TJ, Balsamo G, Berg AA, Boisserie M, Dirmeyer PA, Doblas-Reyes FJ, Drewitt G, Gordon CT, Guo Z, Jeong JH, Lawrence DM, Lee WS, Li Z, Luo L, Malyshev S, Merryfield WJ, Seneviratne SI, Stanelle T, Hurk BJJM, Vitart F, Wood EF (2010) Contribution of land surface initialization to subseasonal forecast skill: first results from a multi-model experiment. Geophys Res Lett 37(L02402):1–6. https://doi.org/10.1029/2009GL041677

Li RL, Bao HY, Li KC, Wang CH (2016) The memory and climate effects of global soil moisture. J Glaciol Geocryol 38(6):1470–1481

Lim KSS, Hong SY (2010) Development of an effective double–moment cloud microphysics scheme with prognostic cloud condensation nuclei (CCN) for weather and climate models. Mon Weather Rev 138:1587–1612

Liu L, Zhang R, Zuo Z (2014) Intercomparison of spring soil moisture among multiple reanalysis data sets over eastern China. J Geophys Res Atmos 119(1):54–64

Liu L, Gu H, Xie J, Xu YP (2021) How well do the ERA-Interim, ERA-5, GLDAS-2.1 and NCEP-R2 reanalysis datasetsrepresent daily air temperature over the Tibetan Plateau? Int J Climatol 41:1484–1505. https://doi.org/10.1002/joc.6867LIUetal.1505

Nicolai-Shaw N, Hirschi M, Mittelbach H, Seneviratne SI (2015) Spatial representativeness of soil moisture using in situ, remote sensing, and land reanalysis data. J Geophys Res Atmos 120:9955–9964. https://doi.org/10.1002/2015JD023305

Ni-Meister W, Walker JP, Houser PR (2005) Soil moisture initialization for climate prediction: characterization of model and observation errors. J Geophys Res 110(110):379–391

Pleim JE (2006) A simple, efficient solution of flux-profile relationships in the atmospheric surface layer. J Appl Meteorol Clim 45:341–347

Pleim (2007) A combined local and non-local closure model for the atmospheric boundary layer. Part 2: application and evaluation in a mesoscale meteorology model. J Appl Meteorol 42(12):1811–1822

Pleim JE, Gilliam R (2009) An indirect data assimilation scheme for deep soil temperature in the Pleim-Xiu Land surface model. J Appl Meteorol Climatol 48(7):1362–1376

Pleim JE, Xiu A (2003) Development of a land surface model. Part II: data Pleim, J. E., 2006: a simple, efficient solution of flux-profile relationships in the atmospheric surface layer. J Appl Meteorol Clim 45:341–347

Prodhomme C, Doblas-Reyes F, Bellprat O, Dutra E (2016) Impact of land-surface initialization on sub-seasonal to seasonal forecasts over Europe. Clim Dyn 47:919–935. https://doi.org/10.1007/s00382-015-2879-4

Seneviratne SI, Koster RD, Guo Z et al (2006a) Soil moisture memory in AGCM simulations: analysis of global land-atmosphere coupling experiment (GLACE) data. J Hydrometeorol 7(5):1090–1112

Seneviratne SI, Luthi D, Litschi M, Schar C (2006b) Land-atmosphere coupling and climate change in Europe. Nature 443(7108):205–209

Seneviratne SI, Corti T, Davin EL et al (2010) Investigating soil moisture–climate interactions in a changing climate: a review. Earth Sci Rev 99(3–4):125–161

Seneviratne SI, Wilhelm M, Stanelle T et al (2013) Impact of soil moisture-climate feedbacks on CMIP5 projections: first results from the GLACE-CMIP5 experiment. Geophys Res Lett 40:5212–5217. https://doi.org/10.1002/grl.50956

Shukla J, Mintz Y (1982) The influence of land-surface evaporation precipitation on earth's climate. Science 215:1498–1501

Song YM, Guo WD, Zhang YC (2009) Numerical study of impacts of soil moisture on the diurnal and seasonal cycles of sensible/latent heat fluxes over semi-arid region. Adv Atmos Sci 26(2):319–326

Vitart F, Buizza R, Balmaseda M et al (2008) The new VAREPS-monthly forecasting system: a first step towards seamless prediction. Q J R Meteorol Soc 134:1789–1799. https://doi.org/10.1002/qj.322

Walker J, Rowntree PR (1977) The effect of soil moisture on circulation and rainfall in a tropical model. Q J R Meteorol Soc 103:29–46

Wang CH, Cui ZQ (2018) Improvement of short-term climate prediction with indirect soil variables assimilation in China. J Clim 31:1399–1412

Wang CH, Dong WJ, Wei ZG (2003) Study on relationship between freezing-thawing processes of the Qinghai–Tibet plateau and the atmospheric circulation over east Asia. Chin J Geophys 46:438–441. https://doi.org/10.1002/cjg2.3361

Wang W, Cui W, Wang X, Chen Xi (2016) Evaluation of GLDAS-1 and GLDAS-2 forcing data and Noah model simulations over China at the monthly scale. J Hydrometeorol 17(11):2815–2833. https://doi.org/10.1175/JHM-D-15-0191.1

Wang CH, Yang K, Zhang FM (2020) Impacts of soil freeze-thaw process and snow melting over Tibetan Plateau on Asian summer monsoon system: a review and perspective. Front Earth Sci 8:133. https://doi.org/10.3389/feart.2020.00133

Wu WR, Marvin AG, Robert ED (2002) The response of soil moisture to long-term variability of precipitation. J Hydrometeorol 3(5):604–613

Yang K, Wang CH (2018) Water storage effect of soil freeze-thaw process and its impacts on soil hydro-thermal regime variations. Agric for Meteorol 265:280–294

Yang K, Wang CH (2019a) Water storage effect of soil freeze-thaw process and its impacts on soil hydro-thermal regime variations. Agric for Meteorol 265:280–294. https://doi.org/10.1016/j.agrformet.2018.11.011

Yang K, Wang CH (2019b) Seasonal persistence of soil moisture anomalies related to freeze–thaw over the Tibetan Plateau and prediction signal of summer precipitation in eastern China. Clim Dyn 53:2411–2424

Yang K, Wang CH, Bao HY (2016) Contribution of soil moisture variability to summer precipitation in the Northern Hemisphere. J Geophys Res Atmos 121:12108–12124. https://doi.org/10.1002/2016JD025644

Yang K, Wang CH, Li SY (2018) Improved simulation of frozen-thawing process in land surface model (CLM4.5). J Geophys Res Atmos 123:13238–13258. https://doi.org/10.1029/2017JD028260

Yeh TC, Wetherald RT, Manable S (1984) The effect of soil moisture on the short-term climate and hydrology change—a numerical experiment. Mon Weather Rev 112:474–490

Zhang T, Barry RG, Knowles K, Ling F, Armstrong R (2003) In: Phillips, Springman, Arenson (eds) Distribution of seasonally and perennially frozen ground in the northern hemisphere. Permafrost, 1289–1294

Zhang J, Wang WC, Wei J (2008) Assessing land-atmosphere coupling using soil moisture from the global land data assimilation system and observational precipitation. J Geophys Res 113:D17119. https://doi.org/10.1029/2008JD009807